Catalytic and conductivity studies in two dimensional coordination polymers built with a thiazole based ligand

Article (Accepted Version)

Catalytic and Conductivity Studies in Two Dimensional Coordination Polymers Built with a Thiazole Based Ligand

Prashant Kumar,*[a,b] Smaragda Lymperopoulou,[a] Edward Loukopoulos,[a] Wakana Matsuda,[b] Nikolaos Kourkoumelis,[c] Shu Seki,*[b] and George E. Kostakis*[a]

[a]Department of Chemistry, School of Life Sciences, University of Sussex, Brighton BN19QJ, UK, E-mail: G.Kostakis@sussex.ac.uk

[b]Department of Molecular Engineering, Graduate School of Engineering, Kyoto University, Nishikyo-ku, Kyoto 615-8510, Japan

E-mail: seki@moleng.kyoto-u.ac.jp; kumar.prashant.25n@st.kyoto-u.ac.jp

[c]Department of Medical Physics, School of Health Sciences, University of Ioannina, 45110 Ioannina, Greece.

Abstract

The employment of the commercial availiable organic ligand 2-mercapto-4-methyl-5-thiazoleacetic acid (H_2L) in Zn and Cd chemistry yields two-dimensional (2D) coordation polymers (CPs) with pseudopolymorphic character. Thermal, catalytic and conductivity studies are discussed.

Keywords: Zinc; Cadmium; Coordination Polymers; Catalysis; Conductivity;

Introduction

Organic ligands bearing several donor atoms (i.e. N, O or S) have been a subject of considerable interest in the field of Chemistry and Material Science during the last few decades. In coordination chemistry, multidentate ligands coordinate to various metals yielding compounds that possess intriguing structural motifs and remarkable properties.[1–4] In the field of advanced materials, the synthetic community shows a preference in the use of five- and six-membered heteroaromatic systems.[5,6] Several compounds based on thiophene and the azole rings have been reported, however the presence of N- and S- atoms in the thiazole five-membered ring gives to the resulting compounds desirable properties.[7] 2-mercapto-4-methyl-5-thiazoleacetic acid (H_2L, Scheme 1) is a hybrid ligand and has five donor atoms (2S, 2O and 1N) exhibiting high versatility and coordination flexibility with a variety of metal ions.[8–10] The different donor sites of heterocyclic thiones can bind with two or more metal ions in order to form metal complexes.[11] Also, the size of the metal anion plays a significant role in the way the metal coordinates to the ligand and as a result in the final polymer's dimensions.[12] H_2L has a very rich chemistry and can find applications in many different aspects. For example, H_2L and some of its coordination complexes

have been found to possess interesting biological properties.[13,14] H_2L has been used for the synthesis of a 40-membered macrocycle containing two distannoxane ladders,[15] and a series of organotin complexes.[16–18] Moreover, H_2L has been used as co-ligand to yield a coordination compound that acts as photosensitizer and can be used in photodynamic therapy,[19] for chemosensor synthesis for determination of heavy metal ions[20] and finally as a stabilizing agent for nanoparticles' (NPs) synthesis for the very same reason.[13,21–23]

From the structural point of view, the reactions of H_2L along with Au^I ion results in a tetranuclear complex, $[Au(LH_2^-)]_4$[24] and three dimers formulated as $[Au(LH_2^-)_2]Cl\cdot 3H_2O$, $Na_3[Au(LH_2)_2]\cdot 6H_2O$ and $Na_3[Au(LH_2)_2]\cdot 10.5H_2O$ with aurophilic interactions and uncommon eclipsed conformation.[25] Moreover, reactions of the ruthenium complexes $[RuH(CO)Cl(PPh_3)_3]$ and $[RuCl_2(PPh_3)_3]$ with H_2L leads two mononuclear complexes formulated as $[RuCl(CO)(PPh_3)_2(H_2L)]$ and $[RuCl(PPh_3)_3(H_2L)]$.[12] The reaction of H_2L with R_3SnCl yields a one dimensional triorganotin carboxylates is formed as $R_3Sn[O_2CCH_2(C_4H_3NS)S]SnR_3$, (R=Me and Ph). [16]

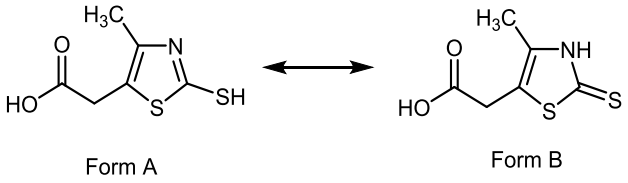

Scheme 1. The protonated forms of the organic ligand 2-mercapto-4-methyl-5-thiazoleacetic acid (H_2L) used in this work.

Organic ligands containing S-atoms have been less used, in contrast to organic ligands that bear N or O atoms, in the field of coordination polymers (CPs), despite their large range of applications such as catalysis, magnetism, gas storage and conductivity.[26] Bearing all these in mind, in this work we have chosen to incorporate the commercial available ligand H_2L along with Zn and Cd salts to form coordination polymers. To the best of our knowledge, this is the first attempt to synthesize CPs with the use of H_2L as the main ligand. We report herein the synthesis, characterization, catalytic and conductivity properties of two compounds formulated as $[Zn^{II}(HL)_2]$ (**1**) and $[Cd^{II}(HL)_2]$ (**2**).

Experimental Section

Materials

Chemicals (reagent grade) were purchased from TCI chemicals and Alfa Aesar. All experiments were performed under aerobic conditions using materials and solvents as received.

Instrumentation

IR spectra of the samples were recorded over the range of 4000–600 cm^{-1} on a Perkin Elmer Spectrum One FT-IR spectrometer (PerkinElmer, Waltham, MA, USA) fitted with an UATR polarization accessory (PerkinElmer). TGA analysis was performed on a TA Instruments Q-50 model (TA, Surrey, UK) under nitrogen, at a scan rate of 20 °C/min. NMR spectra were measured on a Varian VNMRS solution-state spectrometer (Bruker BioSpin, Rheinstetten, Germany) at 500 MHz at 30 °C using residual isotopic solvent ($CDCl_3$, δ_H = 7.24 ppm) as an internal chemical shift reference. Chemical shifts are quoted in ppm. Coupling constants (J) are recorded in Hz. ESI-MS was performed on a VG Autospec Fissions instrument (EI at 70 eV).

X-ray Crystallography. Data for compounds **1** and **2**, were collected (ω-scans) at the University of Sussex using an Agilent Xcalibur Eos Gemini Ultra diffractometer with CCD plate detector under a flow of nitrogen gas at 173(2) K using Cu Kα radiation (λ = 1.54184 Å). CRYSALIS CCD and RED software was used respectively for data collection and processing. Reflection intensities were corrected for absorption by the multi-scan method. All structures were determined using Olex2[27], solved using SHELXT[28] and refined with SHELXL-2014[29]. All non-H atoms were refined with anisotropic thermal parameters, and H-atoms were introduced at calculated positions and allowed to ride on their carrier atoms. In both structures, the H-atom bonded to N on the 5 membered aromatic ring could be located and freely refined, however it was preferred to introduced at calculated position. Crystal data and structure refinement parameters for both compounds are given in Table 1. Geometric/crystallographic calculations were performed using PLATON[30], Olex2[27], and WINGX[31] packages; graphics were prepared with Crystal Maker and MERCURY[32]. Each of the crystal structures has been deposited at the CCDC 1830208 - 1830209.

Table 1. Crystal data and structure refinement for **1** and **2.**

Compound	**1**	**2**
Empirical formula	$C_{12}H_{12}N_2O_4S_4Zn$	$C_{12}H_{12}CdN_2O_4S_4$
Formula weight	441.85	488.88
Temperature/K	173.0	173.0
Crystal system	monoclinic	orthorhombic
Space group	C2/c	Pbca
a/Å	15.5598(8)	14.8393(2)
b/Å	7.4328(5)	14.9312(2)
c/Å	13.7649(8)	15.1186(3)
α/°	90	90
β/°	99.416(6)	90
γ/°	90	90
Volume/$Å^3$	1570.50(16)	3349.82(9)
Z	4	8
$\rho_{calc}g/cm^3$	1.869	1.939
μ/mm^{-1}	7.340	15.291
F(000)	896.0	1936.0

Crystal size/mm^3	0.12 × 0.1 × 0.04	0.14 × 0.1 × 0.06
Radiation	CuKα (λ = 1.54184)	CuKα (λ = 1.54184)
2Θ range for data collection/°	13.04 to 142.89	10.24 to 143.118
Index ranges	$-18 \le h \le 19, -8 \le k \le 8, -16 \le l \le 15$	$-13 \le h \le 18, -18 \le k \le 17, -18 \le l \le 18$
Reflections collected	2365	17294
Independent reflections	1473 [R_{int} = 0.0623, R_{sigma} = 0.1002]	3237 [R_{int} = 0.0423, R_{sigma} = 0.0227]
Data/restraints/parameters	1473/0/106	3237/0/210
Goodness-of-fit on F^2	1.058	1.053
Final R indexes [I>=2σ (I)]	R_1 = 0.0658, wR_2 = 0.1555	R_1 = 0.0366, wR_2 = 0.0956
Final R indexes [all data]	R_1 = 0.0863, wR_2 = 0.1826	R_1 = 0.0375, wR_2 = 0.0967
Largest diff. peak/hole / e $Å^{-3}$	1.18/-0.84	0.70/-1.17

Flash photolysis-time-resolved microwave conductivity (FP-TRMC) measurements.

The charge carrier transporting property in the synthesised 2D CPs was measured by a FP-TRMC technique at room temperature under air. Film samples on a quartz plate were prepared using CP/poly(methylmethacrylate) and dried under vacuum at room temperature. The charge carriers were generated in the prepared film upon direct photoexcitation of CPs by laser pulses of third harmonic generation (λ = 355 nm) from a Nd:YAG laser which corresponds to Spectra Physics model INDI-HG with a pulse duration of 5–8 ns. The photon density of a 355 nm pulse was 9.1 x 10^{15} photons per pulse. The microwave frequency and power were set at ~ 9.1 GHz and 3mW, respectively and The TRMC signal from a diode were recorded by a Tektronix model TDS3032B digital oscilloscope. The complete experimental procedure is mentioned by Seki *et. al*.[33]

Synthetic procedures

Synthesis of (1)

$Zn(NO_3)_2.6H_2O$ (29 mg, 0.1 mmol) was dissolved in 1 ml H_2O and 1 ml DMF and added to a solution of H_2 L (38 mg, 0.2 mmol), (1 ml EtOH and 1 ml DMF). The resulting solution was stirred for 10 min and it was placed in a 25 ml glass vial. This was heated at 90 °C for 24 h and then cooled slowly at room temperature. After cooling at room temperature, colorless crystals were obtained in 65% yield (based on Zn). The crystals were filtered, washed with H_2O, EtOH and Et_2O, and dried in air. Selected IR peaks for (cm^{-1}): 3456 (w), 3017 (m), 2971 (m), 2946 (m), 1739 (s), 1433 (m), 1366 (s), 1229 (s), 1217 (s), 1206 (s), 1112 (w), 1092 (w), 1062 (w), 903 (m), 788 (w), 770 (w), 718 (w), 699 (w). Elemental analysis for $C_{12}H_{12}N_2O_4S_4Zn$: calcd. C 32.62, H 2.74, N 6.34, S 29.03 found C 32.33, H 2.38, N 6.25, S 28.39.

Synthesis of (2)

Compound (**2**) was synthesized in an analogous manner to (**1**) by altering $Zn(NO_3)_2.6H_2O$ with $Cd(NO_3)_2.4H_2O$. After cooling at room temperature, yellowish crystals were obtained in 69% yield

(based on Cd). Selected IR peaks (cm^{-1}): 3453 (w), 3017 (w), 2971 (m), 2945 (w), 1739 (s), 1658 (m), 1554 (s), 1418 (s), 1366 (s), 1229 (s), 1217 (s), 1207 (s), 1105 (w), 1060 (m), 1033 (w), 909 (w), 787 (w), 714 (w), 691 (w). Elemental analysis for $C_{12}H_{12}CdN_2O_4S_4$: calcd. C 29.48, H 2.47, N 5.73, S 26.23 found C 29.25, H 2.52, N 5.67, S 25.45.

Result and Discussion

Crystallographic description

Compound **1** crystallizes in the monoclinic C2/c space group. X-Ray determination of the crystal structure reveals the formation of a neutral two-dimensional (2D) CP (Figure 1, left). The asymmetric unit of **1** consists of a zinc atom on a two-fold rotation axis and one single deprotonated ligand (HL^-). The ligand coordinates to two Zn centres; via one oxygen atom of the carboxylate group and the mercapto S atom (Coordination mode A, Scheme 2). Interestingly, the ligand adopts form B (Scheme 1), however according to the crystallographic data, the two C – S bond lengths are almost equivalent (1.709(6) and 1.716(7)Å) indicating delocalization. The Zn centre adopts a distorted tetrahedral geometry and is coordinated to two O atoms and two S atoms. A detailed list of the bond lengths and angles in **1** is given in Tables S1-2. The compound is a layered structure extending to two dimensions parallel to the *a*0*b* plane. The stability of this architecture is further supported by the formation of several intermolecular interactions; a) a strong intramolecular N-H···O bond between atoms from two different ligands (see Table S5), b) a short intermolecular S···S interaction (see Table S7) and c) weak π-π interactions from adjacent layers (see Table S6).

Compound **2** crystallizes in the orthorhombic Pbca space group. X-Ray determination of the crystal structure reveals the formation of a neutral two-dimensional (2D) CP (Figure 1, right). The asymmetric unit of **2** consists of one Cd centre and two single deprotonated ligands (HL^-). Each ligand coordinates to two Cd centres; via two oxygen atoms of the carboxylate group (chelated) and the mercapto S atom. The ligand adopts form B (Scheme 1), however according to the crystallographic data, the two C – S bond lengths are almost equivalent (1.705(3) and 1.710(3)Å for S1/S2 and 1.704(3) and 1.718(3)Å for S3/S4) indicating delocalization. Interestingly, despite that the two organic ligands adopt the same coordination mode (B, Scheme 2) in the first case the Cd centres is situated above the plane of the 5-memebered ring, where in the second case is placed below the plane. This structural difference has a significant impact in the topological analysis (see below). The Cd centre is coordinated to four O atoms and two S atoms and adopts a pseudo-tetrahedral geometry, if we consider that the two O-atoms of the chelated carboxylate occupy one corner of the tetrahedron. Selected bond lengths and distances for both compounds are given in Tables S3-4. In regards to its architecture, **2** presents a layered structure extending to two dimensions parallel to the *b*0*c* plane. As in the case of **1**, strong intramolecular N-H···O bonds further stabilize the framework. Weak π-π interactions between adjacent layers and short intermolecular S···S distances are also present. As in

1, the adjacent layers in **2** stack following the ABAB pattern along the c axis. The parameters for all these interactions may be found in Tables S1-S10. The topological analysis[34] of the 2D net found in **1** results in the most common **sql** network, whereas the net found in **2** corresponds to a honeycomb (**hcb**) structure. Therefore, compounds **1** and **2**, despite possessing the same molecular formula, they exhibit different topology and thus can be considered as pseudopolymorphs polymers.[35–37]

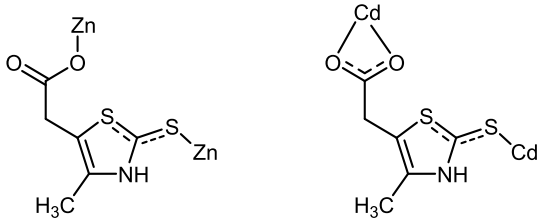

A **B**

Scheme 2. The coordination modes of ligand HL^-, found in compounds **1** (left) and **2** (right).

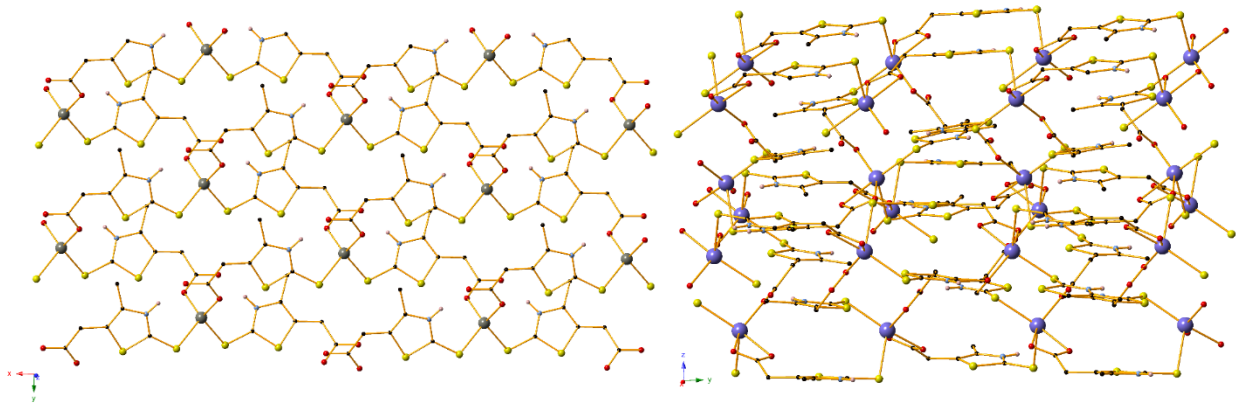

Figure 1. (left) The 2D framework of **1** along the *a*0*b* plane. (right) The 2D framework of **2** along the *b*0*c* plane. Certain H atoms of the structures have been omitted for clarity. Colour code: Zn (grey), Cd (light purple), C (black), H (light pink), N (light blue), O (red), S (yellow).

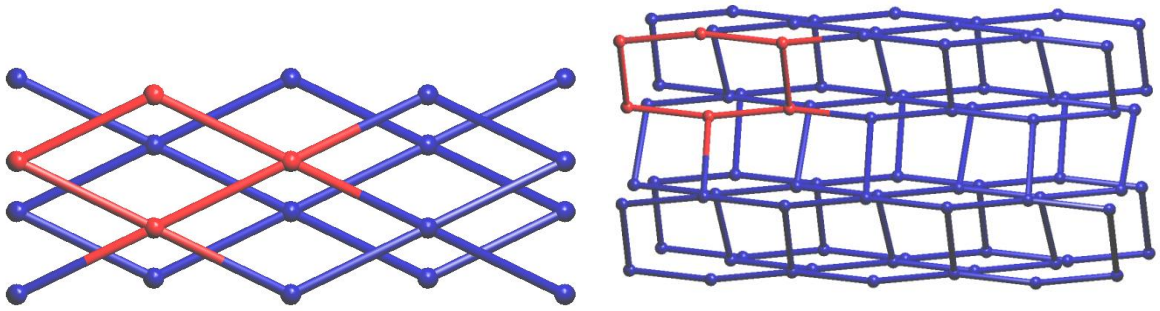

Figure 2. The networks found in **1** (left) and **2** (right).

TGA and PXRD studies.

Both compounds were subjected to thermal analysis in order to study their thermal stability (Figure S1). The results show that both compounds are stable up to 300-320°C because of the absence of

water molecules in their structures. Decomposition starts after this point and is completed at approximately 600°C, indicating the full collapse of the coordination framework. The final residues of these 2D compounds are ZnO for compound (**1**), (observed: 17.96%, calc: 18.42%) and CdO for compound (**2**), (observed: 27.37%, calc: 26.26%). The homogeneity of a bulk crystalline sample from **1** and **2** was confirmed by powder X-ray diffraction. The PXRD patterns of both compounds (Figure 3) were coincide with the simulated PXRD pattern, indicating that the framework is not sensitive upon exposure to air. To assess possible differences between the crystal structure and the powder form of the compounds, Rietveld refinement was performed to the respective powder diffraction patterns. Pseudo-Voigt and FCJ profile functions[38] were used for the fitting approximation of the peak shapes. The background curve was modeled iteratively using polynomial approximation. The U, V and W instrument parameters were also refined, followed structural parameters (coordinates and thermal displacement). The results obtained by Rietveld fit are in good agreement with those obtained by single crystal x-ray data. Specifically, the dimensions of the unit cell for the Zn compound (C2/c) were calculated to a=15.572(2), b=7.443(1), c=13.936(2), b=99.198(6) while for the Cd compound (Pbca) were calculated to a=14.726(3), b=14.905(3), c=15.102(2). Similarly, minimal differences were observed for the atomic positions. The successful refinement is depicted in Figure 3 where the resulted Rietveld fit along with the corresponding figures of merit, profile residual, Rp, and weighted profile residual, wRp, are shown.

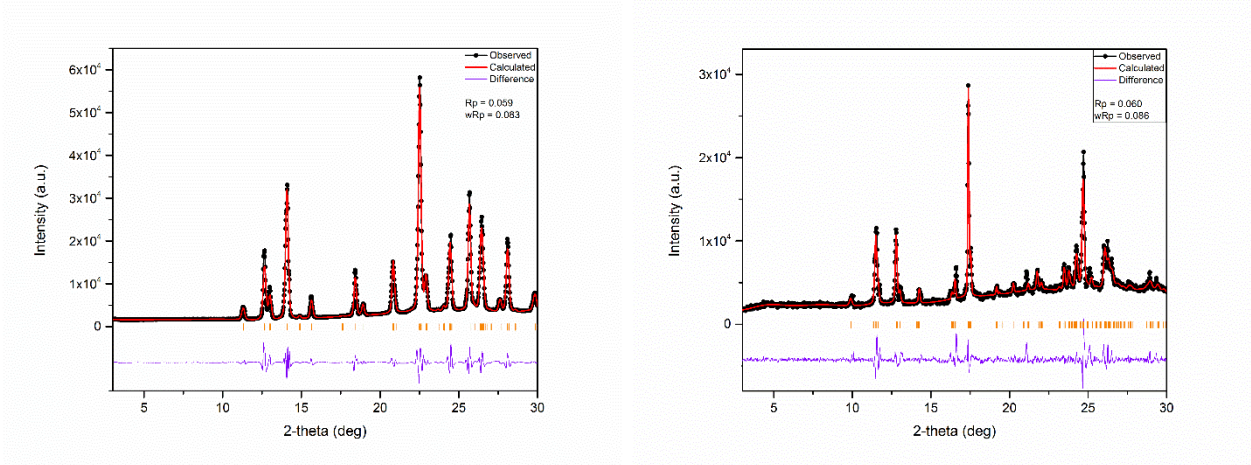

Figure 3. Rietveld refinement to experimental X-ray diffraction pattern for (a) Zn compound (left) Cd compound (right). The vertical ticks indicate the calculated positions of the Bragg peaks.

To exclude the possibility of contamination by an amorphous phase in this sample, SEM observation was performed (Figure S2). The SEM images of the compound **1** and **2** display the presence of homogeneous plate like morphologies.

Catalysis

Some of us have previously used a series of tetranuclear Zn_2Ln_2 coordination clusters as effective Lewis acid catalysts in Friedel-Crafts alkylation of indole with *trans*-β-nitrostyrene.[39] This reaction is poorly promoted by $Zn(OTf)_2$ salt. In this work, given the polymeric nature of both compounds we examined their catalytic activity against the given alkylation reaction, aiming to develop an excellent heterogeneous as well re-usable methodology. Compound **2** does not promote the organic transformation in EtOH, however the reaction proceeds in 100% yield at room temperature after 24 h in ethanol (entry 1, Table 1) when **1** was used in 1.0% loading . Then we examined the catalytic activity of compound **1** in different solvents. The use of different solvents such as THF, water, dichloromethane, chloroform, and DMF (Table 2), give poor or moderate (toluene, entry 5, Table 2) yields. This difference may be attributed to the diffusion limitations of the reactants to reach the active Lewis acid sites or strong binding of solvent (DMF) with the active sites.

Table 2. Scope of the FC alkylation of Indoles with various *trans*-β-nitrostyrene catalysed by **1**[a]

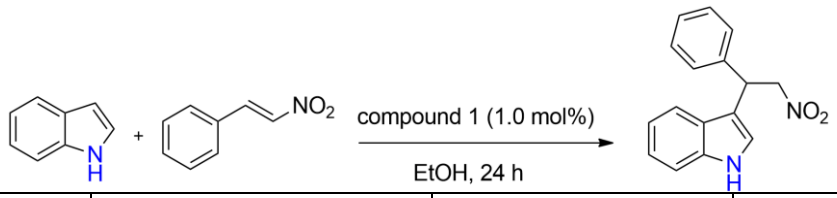

Entry	Solvent	Temperature	Yield (%)[b]
I	**Ethanol**	**r.t**	**100**
II	DMF	r.t	10
III	THF	r.t	16
IV	water	r.t	5
V	toluene	r.t	76
VI	DCM	r.t	20
VII	$CHCl_3$	r.t	26

[a]Reaction conditions: indole (0.2 mmol) with trans-*β*-nitrostyrene (0.2 mmol) in 3 mL of EtOH and 1.0 mol % of compound **1**. [b]Isolated yield by column chromatography.

Having determined the optimal conditions, we extended the scope of the reaction to other substituted nitrostyrenes as well N-methyl-indole (Table 3). The reaction proceeds in excellent yields for unsubstituted indole and N-methylindole (100%) (Table 3). Then, we explored the influence of the substitution in the para position of the aromatic ring in nitrostyrenes (Table 3, entries **4a-4f**). It was found that the *p*-fluoro (F) substitution yields the corresponding product in high yield (100%); however, the use of the *p*-bromo (Br) derivative significantly lowers the yield of the final product. The use of heteroaromatic nitroalkene (Table 3, **4c**) yields the expected product in excellent yield (100 %).

Table 3. FC alkylation of Indoles with various substituted *trans*-β-nitrostyrene catalyzed by compound **1**.[a]

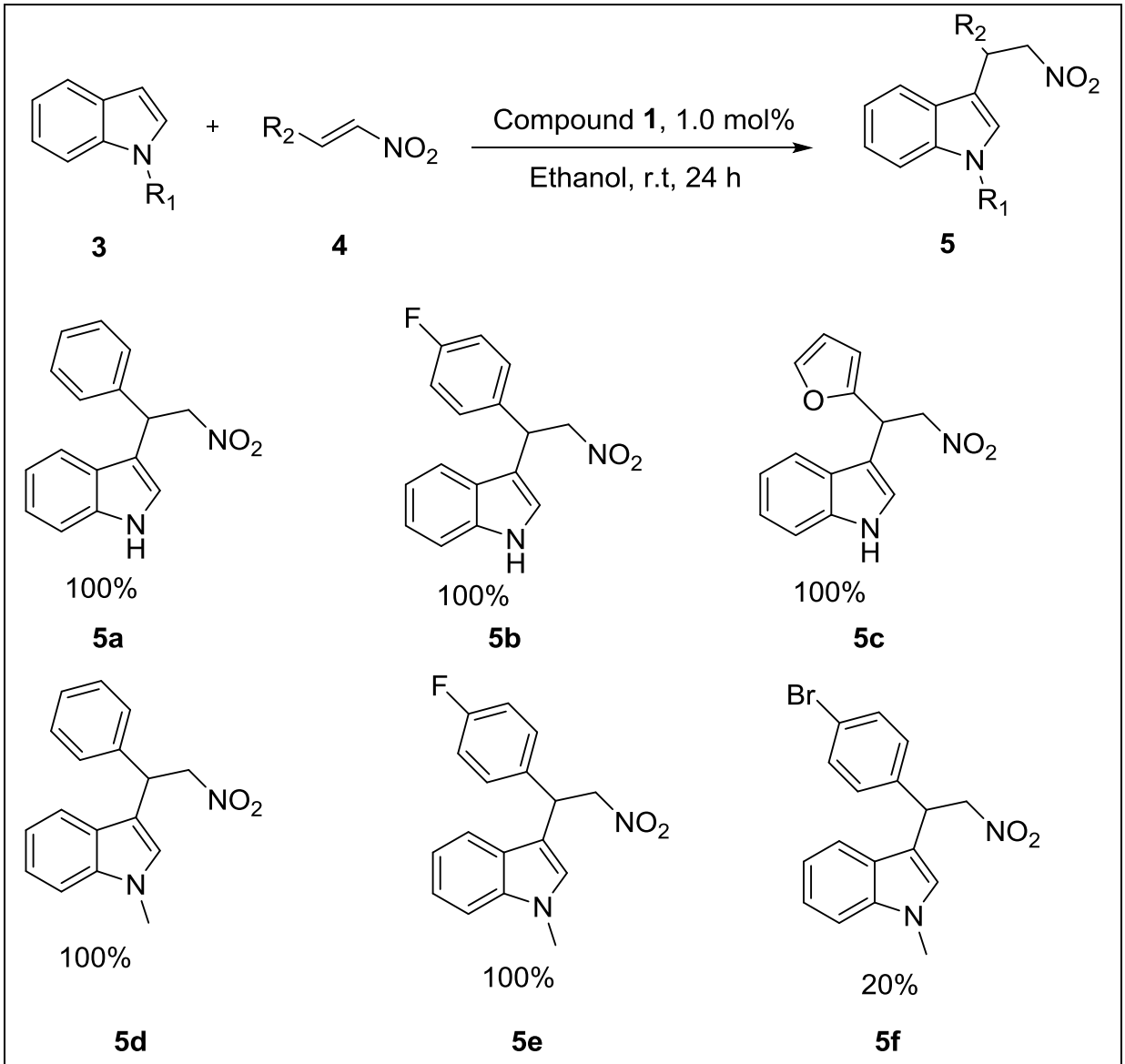

[a]Reaction conditions; indole (0.50 mmol); substituted trans-*β*-nitrostyrene (0.50 mmol); EtOH 5.0 mL; room temperature; 24 h. 1.0% Loading of compound 1.

After catalysis, compound **1** was isolated by filtration, and it was analysed by PXRD. The PXRD pattern (Fig S3-4) showed that the structural integrity was preserved, however minor structural changes could be identified. The use of the recycled catalyst yielded the corresponding product in 100 % (1st cycle), 92 % (2nd cycle) and 86 % (3rd cycle), respectively, therefore it is highly anticipated that the morphology of the catalyst changes upon further use (Figure S4).

Charge-carrier transporting properties

The conductivity of as-synthesized **1** and **2** (Zn and Cd) were determined by flash-photolysis time-resolved microwave conductivity (FP-TRMC) measurement. This technique examines the charge carrier transport properties on the multinanometer length scale that is much smaller than the size of an individual grain or crystallite, and is therefore indicative of the intrinsic charge mobility of a given material.[40] FP-TRMC experiments were performed at room temperature on films made from **1** and **2** bound with poly(methylmethacryrate) as a electronically inactive matrix for the FP-TRMC measurement. The films were placed into a resonant microwave cavity and excited at 355 nm laser light with 5–8 ns pulse duration. The FP-TRMC profiles for as-synthesized CPs **1** and **2** and a similar film made from organic linker H_2L, both shown in Figure 4, show maximum values of $\phi\Sigma\mu$ of 3.9 × 10^{-5} $cm^2/V{\cdot}s$ **1**, and 2.6 × 10^{-5} $cm^2/V{\cdot}s$ **2** respectively, and a long carrier life time where ϕ represent the photocarrier generation yield and $\Sigma\mu$ is the sum of the generated charge carrier mobilities for both electrons and holes. The photo-conductivity kinetic traces decayed principally triple exponential manner; the values are summarized in Table 4. The values in the brackets represent the relative ratio of the decay components. All of the kinetic traces exhibit pseudo-first order ones with long enough lifetimes as represented by k_3 of 4.2 -5.0 × 10^4 s^{-1} (τ ~ 20 - 24 μs), suggesting that the signals were observed as the transient conductivity of free charge carriers after geminate charge recombination processes.

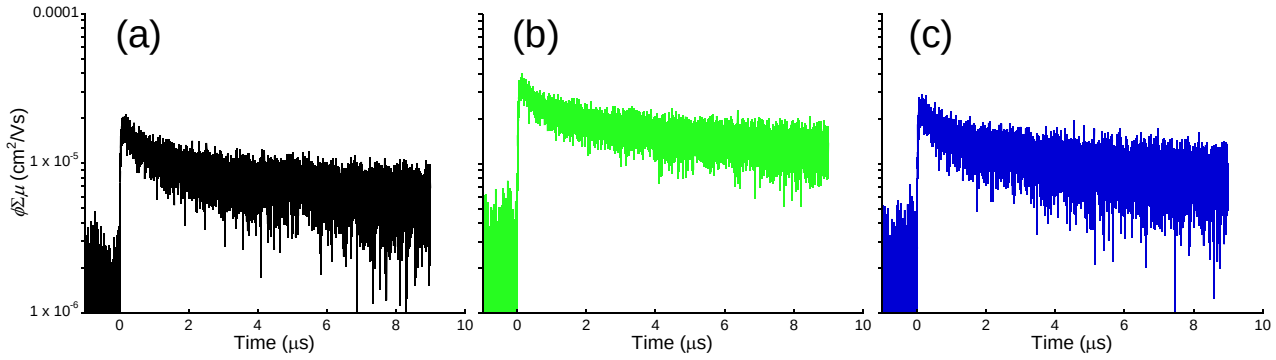

Figure 4. Conductivity transients observed by FP-TRMC of H_2L (black trace, a), Zn - CP **1** (green trace, b) and Cd – CP **2** (blue trace, c) after laser pulse excitation at 355 nm with 9.1 × 10^{15} photons cm^{-2} $pulse^{-1}$

Table 4. Kinetics of the Photoconductivity Decay

Compound	k_1 (s^{-1})	k_2 (s^{-1})	k_3 (s^{-1})
1	1.8 × 10^6 (0.45)[a]	9.5 × 10^4 (0.2)	5.0 × 10^4 (0.35)
2	1.8 × 10^6 (0.45)	7.0 × 10^4 (0.4)	5.0 × 10^4 (0.15)
H_2L	1.6 × 10^6 (0.52)	7.0 × 10^4 (0.43)	4.2 × 10^4 (0.05)

[a]The values in the brackets represent the relative ratio of the decay components

Focusing onto the contribution from the photo-generated free charge carriers as $(\phi\Sigma\mu)_{max} \times (k_3$ ratio), **1** marked 3-hold higher value than that in **2**. Most importantly, the S···S intermolecular distance observed in **1** and **2** increases from 3.303(2) Å in **1** to 3.6878(11) Å in **2** (Table S7-S10). This difference may be attributed to the different ionic radii of Cd^{2+}(109 pm) when compared with Zn^{2+} (88 ppm), and thus **1** that exhibits the shortest S···S distance shows higher conductivity. This explanation suggests that shortening the length of the intermolecular S···S contacts, even higher charge mobility can be obtained, therefore our future studies will be focusing towards this direction.

Conclusions

The first examples of 2D CPs built from 2-mercapto-4-methyl-5-thiazoleacetic acid and Zn and Cd metal centres are reported. The new compounds show interesting structural features (pseudopolymorphism). Compound **1** was found to act as an efficient Lewis acid catalyst towards the Friedel-Crafts alkylation of nitrostyrene-indole. Along with catalysis, we have shown the use of the thiazole based ligand yields stable, non-sensitive upon exposure to air, CPs that exhibit moderate conductivity determined by FP-TRMC.

Acknowledgments

P. K. and S. S. are thankful to the Japan Society for the Promotion of Science (JSPS, P16342 for a fellowship, 26102011, and 15K21721). S. L. acknowledges support from the program LLP Erasmus Placements. G.E.K. thanks the EPSRC (UK) for funding (grant number EP/M023834/1).

Appendix A. Supplementary data

CCDC 1830208 – 1830209 contains the supplementary crystallographic data for **1** and **2**. These data can be obtained free of charge via http://www.ccdc.cam.ac.uk/conts/retrieving.html, or from the Cambridge Crystallographic Data Centre, 12 Union Road, Cambridge CB2 1EZ, UK; fax: (+44) 1223-336-033; or e-mail: deposit@ccdc.cam.ac.uk.

References

[1] P. Abbasi, K. Quinn, D.I. Alexandropoulos, M. Damjanović, W. Wernsdorfer, A. Escuer, J. Mayans, M. Pilkington, T.C. Stamatatos, Transition Metal Single-Molecule Magnets: A {Mn31} Nanosized Cluster with a Large Energy Barrier of ~60 K and Magnetic Hysteresis at ~5 K, J. Am. Chem. Soc. 139 (2017) 15644–15647. doi:10.1021/jacs.7b10130.

[2] G. Maayan, N. Gluz, G. Christou, A bioinspired soluble manganese cluster as a water oxidation electrocatalyst with low overpotential, Nat. Catal. 1 (2018) 48–54. doi:10.1038/s41929-017-0004-2.

[3] A. Baniodeh, N. Magnani, Y. Lan, G. Buth, C.E. Anson, J. Richter, M. Affronte, J. Schnack, A.K. Powell, High spin cycles: topping the spin record for a single molecule verging on quantum criticality, Npj Quantum Mater. 3 (2018) 10. doi:10.1038/s41535-018-0082-7.

[4] R.L. Siegelman, T.M. McDonald, M.I. Gonzalez, J.D. Martell, P.J. Milner, J.A. Mason, A.H. Berger, A.S. Bhown, J.R. Long, Controlling Cooperative CO2 Adsorption in Diamine-Appended Mg2(dobpdc) Metal-Organic Frameworks, J. Am. Chem. Soc. 139 (2017) 10526–10538. doi:10.1021/jacs.7b05858.

[5] F. Shibahara, E. Yamaguchi, T. Murai, Direct arylation of simple azoles catalyzed by 1,10-phenanthroline containing palladium complexes: An investigation of C4 arylation of azoles and the synthesis of triarylated azoles by sequential arylation, J. Org. Chem. 76 (2011) 2680–2693. doi:10.1021/jo200067y.

[6] A. Mori, A. Sugie, Palladium-catalyzed CH arylation and dehydrogenative homocoupling of heteroaromatic compounds and application to the design of advanced organic materials, Bull. Chem. Soc. Jpn. 81 (2008) 548–561. doi:10.1246/bcsj.81.548.

[7] B. Ustamehmetoğlu, Synthesis and Characterization of Thiophene and Thiazole Containing Polymers, Electrochim. Acta. 122 (2014) 130–140. doi:10.1016/j.electacta.2013.12.130.

[8] S. Chandra, L.K. Gupta, Sangeetika, Spectroscopic, cyclic voltammetric and biological studies of transition metal complexes with mixed nitrogen-sulphur (NS) donor macrocyclic ligand derived from thiosemicarbazide, Spectrochim. Acta - Part A Mol. Biomol. Spectrosc. 62 (2005) 453–460. doi:10.1016/j.saa.2005.01.015.

[9] S.H. and M.C.R. de A. and P.G.J. J. Vicente, M. Chicote, Synthesis and Structural Characterization of Gold (I) and Silver (I) Complexes of the Multidonor Ligand 2-(Phenacylthio)pyridine Crystal Structures of {py{SCH2C(O)Ph}-2}], Eur. J. Inorg. Chem. (1998) 511–516.

[10] L.M. Brines, J. Shearer, J.K. Fender, D. Schweitzer, S.C. Shoner, D. Barnhart, W. Kaminsky, S. Lovell, J.A. Kovacs, Periodic Trends within a Series of Five-Coordinate Thiolate-Ligated [M II (S Me2 N 4 (tren))] + (M) Mn , Fe , Co , Ni , Cu , Zn) Complexes , Including a Rare Example of a Stable Cu II − Thiolate, Inorg. Chem. 46 (2007) 9267–9277.

[11] H. Tannai, K. Tsuge, Y. Sasaki, O. Hatozaki, N. Oyama, Monodentate and bridging coordination of 2,5-dimercapto-1,3,4-thiadiazolate to a (2,2′:6′,2″-terpyridine)platinum(II) center, Dalt. Trans. (2003) 2353–2358.

[12] P. Kumar, M. Yadav, A.K. Singh, D.S. Pandey, Synthesis and characterization of some novel ruthenium(II) complexes containing thiolate ligands, J. Organomet. Chem. 695 (2010) 994–1001. doi:10.1016/j.jorganchem.2009.12.006.

[13] P. Kannan, S.A. John, Highly sensitive determination of hydroxylamine using fused gold

nanoparticles immobilized on sol-gel film modified gold electrode, Anal. Chim. Acta. 663 (2010) 158–164. doi:10.1016/j.aca.2010.01.045.

[14] P. Kannan, S.A. John, Highly sensitive electrochemical determination of nitric oxide using fused spherical gold nanoparticles modified ITO electrode, Electrochim. Acta. 55 (2010) 3497–3503. doi:10.1016/j.electacta.2010.01.084.

[15] C. Ma, J. Sun, A novel self-assembling synthesis and crystal structure of 40-membered macrocyclic complex containing eight-tin., Dalt. Trans. (2004) 1785–1786. doi:10.1039/B405247A.

[16] C. Ma, J. Sun, L. Qiu, J. Cui, The synthesis and characterization of triorganotin carboxylates of 2-Mercapto-4-methyl-5-thiazoleacetic acid: X-ray crystal structures of polymeric Me3Sn[O2CCH2(C4H 3NS)S]SnMe3 and Ph3Sn[O2CCH 2(C4H3NS)S]SnPh3, J. Inorg. Organomet. Polym. 15 (2005) 341–347. doi:10.1007/s10904-005-7875-4.

[17] R. Zhang, J. Sun, C. Ma, Synthesis and crystal structure of macrocyclic di-n-butyltin(IV) complex with 2-mercapto-4-methyl-5-thiazoleacetic acid, {[n-Bu2Sn(O2CCH2C4H3NS)SS(C4H3NSCH2CO2)Sn n-Bu2]O}2, Inorganica Chim. Acta. 357 (2004) 4322–4326. doi:10.1016/j.ica.2004.06.026.

[18] R.F. Zhang, J.F. Sun, C.L. Ma, J.H. Zhang, Synthesis, Characterization and Crystal Structures of Diorganotin(IV) Complexes with 2-Mercapto-4-methyl-5-thiazoleacetic Acid, Pol. J. Chem. 80 (2006) 367–376.

[19] S. Moeno, E. Antunes, S. Khene, C. Litwinski, T. Nyokong, The effect of substituents on the photoinduced energy transfer between CdTe quantum dots and mercapto substituted zinc phthalocyanine derivatives., Dalt. Trans. 39 (2010) 3460–3471. doi:10.1039/b926535j.

[20] A.A.A. Hamid, C.P. Tripp, A.E. Bruce, M.R.M. Bruce, Application of structural analogs of dimercaptosuccinic acid-functionalized silica nanoparticles (DMSA- silica) to adsorption of mercury, cadmium, and lead, Res. Chem. Intermed. 37 (2011) 791–810. doi:10.1007/s11164-011-0317-8.

[21] N. Vasimalai, S.A. John, Off-on and on-off chemosensors for ultratrace mercury(II) and copper(II) using functionalized thiazole and cadmium sulfide nanoparticles fluorophores, Sensors Actuators, B Chem. 190 (2014) 800–808. doi:10.1016/j.snb.2013.09.028.

[22] P. Kannan, S.A. John, Synthesis, Characterization and Electrocatalytic Activity of Fused Gold Nanoparticles, J. Nanosci. Nanotechnol. 11 (2011) 2142–2150. doi:10.1166/jnn.2011.3561.

[23] Y. Su, Y. Lin, Y. Fu, F. Qian, X. Yang, M.M.F. Choi, Synthesis and Characterization of Water-Soluble Monolayer-Protected Gold Nanoparticles, Adv. Mater. Res. 415–417 (2011) 617–620. doi:10.4028/www.scientific.net/AMR.415-417.617.

[24] B. Tzeng, W. Liu, J. Liao, G. Lee, S. Peng, Self-Assembly of Gold (I) Compounds with 2004,

Cryst. Growth Des. 4 (2004) 573–577.

[25] M. Hapka, M. Dranka, K. Orłowska, G. Chałasinski, M.M. Szczesniak, J. Zachara, Noncovalent interactions determine the conformation of aurophilic salts with 2-Mercapto-4-methyl-5-thiazoleacetic acid ligands †, Dalt. Trans. 44 (2015) 13641–13650. doi:10.1039/b000000x.

[26] E.J. Mensforth, M.R. Hill, S.R. Batten, Coordination polymers of sulphur-donor ligands, Inorg Chim Acta. 403 (2013) 9–24. doi:10.1016/j.ica.2013.02.019.

[27] O. V Dolomanov, A.J. Blake, N.R. Champness, M. Schröder, OLEX: New software for visualization and analysis of extended crystal structures, J. Appl. Crystallogr. 36 (2003) 1283–1284.

[28] G.M. Sheldrick, SHELXT – Integrated space-group and crystal-structure determination, Acta Crystallogr. Sect. A Found. Adv. 71 (2015) 3–8. doi:10.1107/S2053273314026370.

[29] G.M. Sheldrick, A short history of SHELX, Acta Crystallogr. Sect. A. 64 (2008) 112–122. doi:10.1107/s0108767307043930.

[30] A.L. Spek, Single-crystal structure validation with the program PLATON, J. Appl. Crystallogr. 36 (2003) 7–13. doi:10.1107/S0021889802022112.

[31] L.J. Farrugia, suite for small-molecule single-crystal crystallography, J. Appl. Crystallogr. 32 (1999) 837–838. doi:10.1107/S0021889899006020.

[32] C.F. Macrae, P.R. Edgington, P. McCabe, E. Pidcock, G.P. Shields, R. Taylor, M. Towler, J. Van De Streek, Mercury: Visualization and analysis of crystal structures, J. Appl. Crystallogr. 39 (2006) 453–457. doi:10.1107/S002188980600731X.

[33] F.C. Grozema, L.D.A. Siebbeles, J.M. Warman, S. Seki, S. Tagawa, U. Scherf, Hole conduction along molecular wires: α-bonded silicon versus π-bond-conjugated carbon, Adv. Mater. 14 (2002) 228–231. doi:10.1002/1521-4095(20020205)14:3<228::AID-ADMA228>3.0.CO;2-3.

[34] V.A. Blatov, A.P. Shevchenko, D.M. Proserpio, Applied Topological Analysis of Crystal Structures with the Program Package ToposPro, Cryst. Growth Des. 14 (2014) 3576–3586. doi:10.1021/cg500498k.

[35] V.N. Dokorou, A.K. Powell, G.E. Kostakis, Two pseudopolymorphs derived from alkaline earth metals and the pseudopeptidic ligand trimesoyl-tris-glycine, Polyhedron. 52 (2013) 538–544. doi:10.1016/j.poly.2012.08.032.

[36] C.N. Morrison, A.K. Powell, G.E. Kostakis, Influence of Metal Ion on Structural Motif in Coordination Polymers of the Pseudopeptidic Ligand Terephthaloyl-bis-beta-alaninate, Cryst. Growth Des. 11 (2011) 3653–3662. doi:10.1021/cg2007028.

[37] H.H. Monfared, A.-C.C. Chamayou, S. Khajeh, C. Janiak, Can a small amount of crystal

solvent be overlooked or have no structural effect? Isomorphous non-stoichiometric hydrates (pseudo-polymorphs): the case of salicylaldehyde thiosemicarbazone, CrystEngComm. 12 (2010) 3526–3530. doi:10.1039/c0ce00041h.

[38] L.W. Finger, D.E. Cox, A.P. Jephcoat, IUCr, A correction for powder diffraction peak asymmetry due to axial divergence, J. Appl. Crystallogr. 27 (1994) 892–900. doi:10.1107/S0021889894004218.

[39] P. Kumar, S. Lymperopoulou, K. Griffiths, S.I. Sampani, G.E. Kostakis, Highly efficient tetranuclear ZnII2LnIII2 catalysts for the Friedel – Crafts alkylation of indoles and nitrostyrenes, Catalysts. 6 (2016) 140.

[40] A. Saeki, Y. Koizumi, T. Aida, S. Seki, Comprehensive approach to intrinsic charge carrier mobility in conjugated organic molecules, macromolecules, and supramolecular architectures, Acc. Chem. Res. 45 (2012) 1193–1202. doi:10.1021/ar200283b.